Current Biology, Vol. 14, 2107–2112, December 14, 2004, ©2004 Elsevier Ltd. All rights reserved. DOI 10.1016/j.cub.2004.11.051

Chromosome Fragmentation after Induction of a Double-Strand Break Is an Active Process Prevented by the RMX Repair Complex

Kirill Lobachev,[1,3] Eric Vitriol,[2] Jennifer Stemple,[2] Michael A. Resnick,[1,4,*] and Kerry Bloom[2,4,*]
[1]Laboratory of Molecular Genetics
National Institute of Environmental Health Sciences
National Institutes of Health
101 Alexander Drive
Research Triangle Park, North Carolina 27709
[2]Department of Biology
University of North Carolina at Chapel Hill
Call Box #3280
623 Fordham Hall
Chapel Hill, North Carolina 27599
[3]School of Biology
Institute for Bioengineering and Bioscience
Georgia Institute of Technology
Atlanta, Georgia 30332

Summary

Chromosome aberrations are common outcomes of exposure to DNA-damaging agents or altered replication events and are associated with various diseases and a variety of carcinomas, including leukemias, lymphomas, sarcomas, and epithelial tumors [1, 2]. The incidence of aberrations can be greatly increased as a result of defects in DNA repair pathways [3]. Although there is considerable information about the molecular events associated with the induction and repair of a double-strand break (DSB), little is known about the events that ultimately lead to translocations or deletions through the formation of chromosome breaks or the dissociation of broken ends. We describe a system for visualizing DNA ends at the site of a DSB in living cells. After induction of the break, DNA ends flanking the DSB site in wild-type cells remained adjacent. Loss of a functional RMX complex (Rad50/Mre11/Xrs2) or a mutation in the Rad50 Zn-hook structure resulted in DNA ends being dispersed in approximately 10%–20% of cells. Thus, the RMX complex holds broken ends together and counteracts mitotic spindle forces that can be destructive to damaged chromosomes.

Results

A target site for the homing endonuclease I-SceI was created on the right arm of chromosome II and flanked by the lactose and tetracycline operator arrays. The operator arrays were visualized upon binding of lacI-GFP (green fluorescent protein) and tetR-CFP (cyan fluorescent protein), respectively. Spindle poles were visualized with the spindle pole component (SPC29) fused to red fluorescent protein (RFP) (Figure 1). LacO and tetR foci remain adjacent throughout the cell cycle. Thus, microtubule-based forces encountered during mitosis and anaphase spindle elongation do not disrupt repressor-operator interactions.

Induction of the I-SceI endonuclease led to the appearance of a DSB in 50% and 90% of chromosome II at 2 and 6 hr, respectively, for the wild-type strain (see Figure S1A in the Supplemental Data available with this article online) and 65%–70% and 90% of *yku70* and *mre11*Δ cells at 2 and 6 hr, respectively (Figure S1A). Loss of the 3.7 and 3.1 I-SceI cleavage products in wild-type and y*ku70*Δ mutants reflects DNA end processing. Among the cleavage products in *mre11*Δ, 32% experienced no degradation at 6 hr, consistent with the proposed role for RMX in end processing (reviewed in Haber, [4]).

The fraction of DSBs was confirmed through direct analysis of chromosomes by transverse alternating field electrophoresis (TAFE). Induction of I-SceI resulted in 50% loss of intact chromosome II for the wild-type and 60% for the *mre11* mutant at 2 hr of induction. Southern analysis of the TAFE gel revealed a single I-SceI cut site in chromosome II (Figure S1B). The loss of intact chromosome II extends and confirms the fraction of DSBs estimated by Southern analysis (Figure S1A).

Induction of a DSB Leads to the Accumulation of Large-Budded Cells with Mitotic Spindles

A single irreparable DSB has been shown to arrest cell cycle progression in G2/M [5]. Upon induction of I-SceI, the fraction of large-budded cells increased from ~30% of the population in uninduced cells to over 85% in wild-type cells (shaded bars, Figure S1B). Less than 5% of arrested cells (containing spindles <4.0 μm) had two lacI or tetR foci after 2 and 6 hr of I-SceI induction (Figure S2). The predominance of single foci reflects the lack of sister chromatid separation during the mitotic arrest. The observation that approximately 50% and 90% of the DNA was broken at 2 hr and 6, respectively, suggests that the maximum number of cells with breaks in both sister chromatids is approximately 25% and 80% (the product of the individual probabilities at each time point).

Lack of Chromosome Fragmentation in Wild-Type Cells

The 15 kb of DNA between the two operators can expand and contract, leading to transient foci separations in living cells. In the absence of I-SceI induction, tetR-CFP and lacI-GFP foci were coincident or separated by <0.8 μm at all stages of cell cycle progression (Figures 1 and 2; wild-type cells; $n > 400$ cells). Upon induction of I-SceI endonuclease, tetR-CFP and lacI-GFP foci remained coincident in wild-type cells (>98% coincident or separated by less than 0.8 μm; $n = 400$ cells). Sixty to seventy percent of wild-type and mutant cells contained both foci, indicating that the ability to detect chromosome

*Correspondence: kbloom@email.unc.edu (K.B.); resnick@niehs.nih.gov (M.A.R.)
[4]These authors contributed equally to this work.

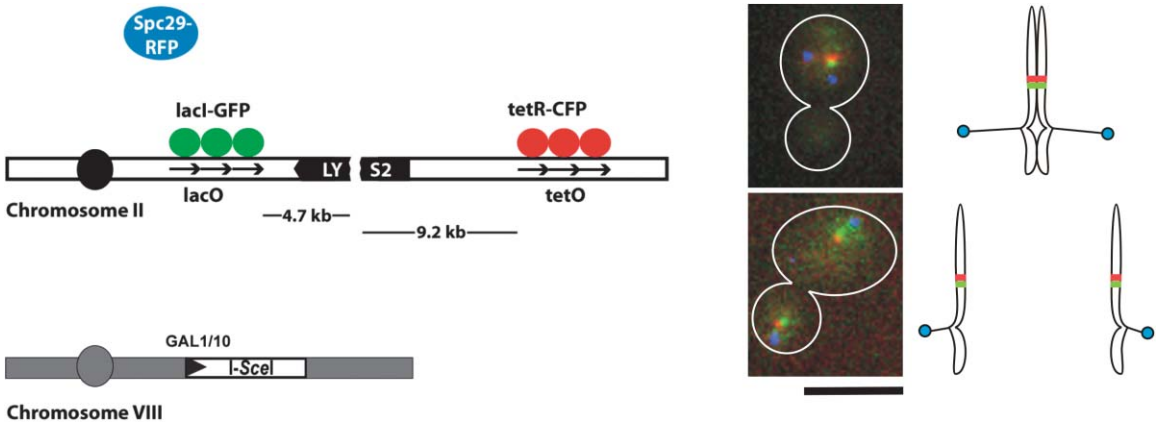

Figure 1. System to Detect the Induction of a Chromosome Break by a Single DSB in Haploid Yeast

An I-SceI site is present in the *LYS2* gene on chromosome II; the distances from lacO and tetO arrays to I-SceI cutting position on chromosome II are indicated (left). A *GALI*::I-SceI cassette is integrated into chromosome VIII (see Supplemental Experimental Procedures). The lacI-GFP (green ovals) and tetR-CFP (red ovals) hybrid proteins are shown bound to lacO and tetO arrays (arrows), respectively. The blue oval indicates spindle poles that can be visualized via fusion of spindle pole protein Spc29 with RFP. The images at right are a microscopic visualization of lacI-GFP (green spot), tetR-CFP (red spot), and Spc29-RFP (two blue spots) foci in large-budded cells in the absence of I-SceI induction. Presented are examples of cells in early anaphase before sister chromatid separation (fluorescence, upper left; schematic, upper right) and cells in late anaphase after sister chromatid separation (fluorescence, lower left; schematic, lower right). In the absence of I-SceI induction, the lacI-GFP and tetR-CFP foci are coincident or separated by <0.8 μm. The scale bar represents 5 μm.

breaks is not compromised by resection of DNA strands at DSB sites. Thus, physical separation of DNA ends does not accompany double-strand breakage in wild-type cells. The lack of transition from a DSB to a chromosome break led us to examine whether proteins associated with the ends of the broken molecules prevent chromosome fragmentation.

Chromosome Fragmentation in Mutants of the RMX Complex

Induction of I-SceI in *mre11*Δ mutants led to the accumulation of large-budded cells with short mitotic spindles at 2 and 6 hr (<4 μm; Figure S1B). Approximately 12% of large-budded cells exhibited chromosome breaks (CRBs), as determined by tetR-CFP and lacI-GFP foci separated by distances greater than 0.8 μm (Figures 2 and 3). The foci displacements ranged between 0.8 and 5 μm (Figure 3, upper left). Similar fractions of separated tetR-CFP and lacI-GFP spots were found in cells lacking *rad50*, *xrs2*, or *mre11* (Figure 2). Thus, the increase in chromosome fragmentation reflects loss of any component of the RMX complex. The absence of *dnl4* along with *mre11* or *rad50* resulted in a similar fraction of separated foci (8%–9%; Figure 2). This finding rules out the possibility that DSBs are repaired at later time points in the single mutants.

To identify the critical function of RMX in preventing chromosome fragmentation, we examined foci separation in *rad50* mutants carrying amino acid changes in the CXXC zinc-hook motif [6] and in *mre11* nuclease-defective mutants [7, 8]. Chromosome breaks were detected in less than ~1% of the nuclease mutants, indicating that the nuclease activity of Mre11p is not required to prevent chromosome breakage (Figure 2). The Zn-hook domain, which is located at the apex of the Rad50 coiled-coil domain, has been proposed as a link between RMX complexes bound to DNA ends. *rad50* hook mutants exhibited significant increases in separated foci upon I-SceI induction. Ten and seventeen percent of *rad50*-C1G cells and 20% and 5% of *rad50*-C2S cells contained separated foci at 2 hr and 6 hr, respectively. The decrease in separated foci at 6 hr in the *rad50*-C2S mutants may reflect lacI-GFP or tetR-CFP loss owing to end resection (approximately 50% fewer cells with both foci than *rad50*-C1G; E.V. and K.B., unpublished data) or other processing events that would lead to loss of operator binding sites and limit the visualization of two spots. In either case, the increase in spot separation in RMX mutants provides in vivo evidence for a proposed role of this complex in tethering DNA molecules [9].

Foci were examined in *yku70* mutants to determine whether other proteins involved in end joining might prevent chromosome breakage. tetR-CFP and lacI-GFP foci were coincident at 0 time and after 2 hr of I-SceI induction (Figure 2; *yku70*, $n > 300$ cells). At 6 hr, there was a small but not statistically significant increase in separated foci (3%; *yku70* 7/216; $p = 0.28$; Table S1). Similarly, there was no significant induction of separated foci in a *dnl4*Δ mutant (1/176) required for the ligation step of nonhomologous end joining (NHEJ) (reviewed in [10]). Thus, proteins involved specifically in end joining are not required for preventing chromosome breakage at sites of DSB.

Chromosome Fragmentation Can Lead to Loss of the Acentric Fragment

Separated foci were found in three distinct configurations. Two hundred seven of two hundred forty cells (86.5%) with separated spots were arrested prior to anaphase onset with short spindles and unseparated sister chromatids (Figure 3; Figure S2). The distance separating tetR-CFP and lacI-GFP spots (Figure 3, upper left) often exceeded the distance between spindle poles (2–4 μm, Scp29-RFP). These data indicate that once broken,

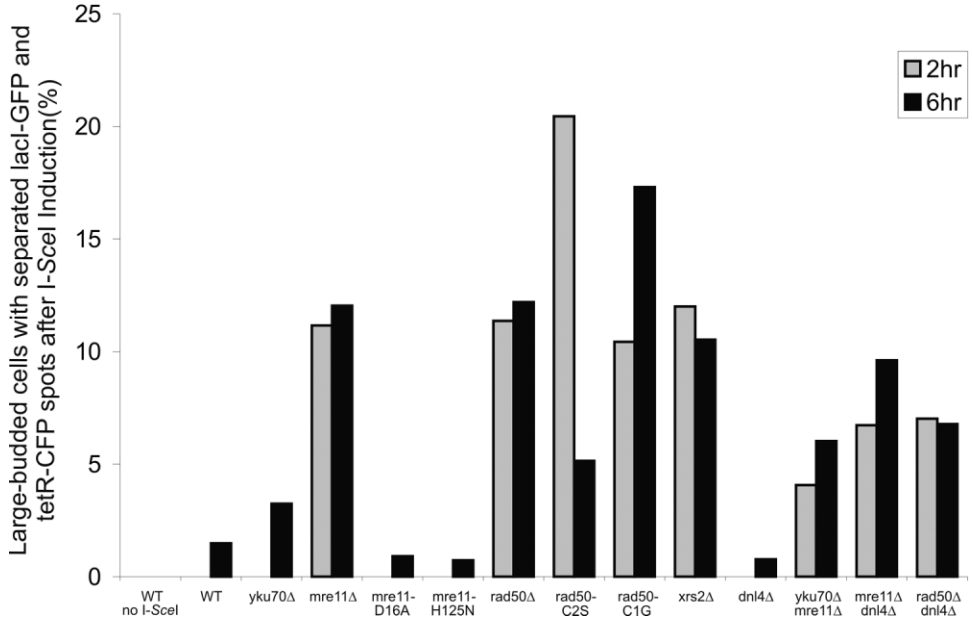

Figure 2. Separation of tetR-CFP and lacI-GFP Spots after Induction of I-SceI

I-SceI was induced by transfer to galactose-containing media for 0, 2, and 6 hr.

(A) The fraction of large budded cells containing tetR-CFP and lacI-GFP spots separated by greater than 0.80 μm was determined. The instances of spot separations are as follows (at 2hr and 6hr): wild-type without *GAL1*::I-SceI cassette, 0/100, 0/100; wild-type, 0/160, 3/135; *yku70*Δ, 0/100, 7/216; *mre11*Δ, 27/252, 13/108; *mre11*-D16A, 0/103, 1/110; *mre11*-H125N, 0/129, 1/129; *rad50*Δ, 15/132, 15/123; *rad50*-C2S, 36/176, 9/176; *rad50*-C1G, 12/116, 18/104; *xrs2*Δ, 15/125, 12/124; *dnl4*Δ, 0/119, 1/176; *yku*70Δ *mre*11Δ, 5/123, 9/126; *mre11*Δ *dnl4*Δ, 7/104, 10/104; and *rad50*Δ *dnl4*Δ, 8/114, 8/118. At 0 hr of I-SceI induction, tetR-CFP and lacI-GFP spots were always coincident for all mutant strains.

both chromosome fragments may no longer be tethered to the mitotic spindle (see below).

In approximately 10% of cells with separated spots (23/240), two tetR-CFP and lacI-GFP spots could be observed. An example of this configuration is shown in Figure 3 (upper right). One of the tetR-CFP and lacI-GFP pairs was overlapping near the bottom spindle pole (left panel); the other tetR-CFP and lacI-GFP pair (upper spindle pole) were separated by approximately 1.3 μm (middle and right panels, Figure 3). The cell is in anaphase, as indicated by the increased distance between spindle poles (~5.5 μm) and separated sister chromatids. The progression into anaphase in approximately 10% of cells provides the opportunity to visualize chromosome breaks in one of the sister chromatids. Sister chromatid cohesion would likely prevent fragmentation if only one sister has experienced a break. However, upon loss of cohesion in anaphase, chromosome breaks are readily apparent (Figure 3).

The third configuration reflects loss of an acentric fragment. These cells also contain four distinct foci (Figure 3; 4.2% of cells with separated spots; 10/240). The lacI-GFP spots marking the centromere-containing chromosome fragment segregated to opposite spindle poles (lower right, Figure 3). In contrast, the tetR-CFP acentric fragment separated but failed to segregate to opposite poles upon anaphase onset (Figure 3). These results provide direct evidence for loss of an acentric chromosome fragment after induction of a DSB.

Centric versus Acentric Chromosome Dynamics

The mitotic spindle is a highly dynamic structure that often makes excursions between the mother and daughter of mitotic arrested cells [11]. Chromosomes remain associated with the spindle throughout these movements. Chromosome dynamics in live cells, therefore, provide a powerful assay to establish whether the acentric fragment remains tethered to the spindle. The behavior of separated tetR-CFP and lacI-GFP foci in RMX mutant cells was analyzed by time-lapse fluorescence microscopy. Selected frames over a 15 min time course are shown in Figure 4. The centromere fragment (lacI-GFP, green) remained within a 0.25 μm cylinder surrounding the mitotic spindle (Figure 4). The spindle was dynamic, making excursions between the mother and bud at rates consistent with microtubule-based motility. The spindle did not change in length during the arrest. In cells with overlapping tetR-CFP and lacI-GFP foci, both foci behaved as the centromere fragment shown in Figure 4 (data not shown). The acentric fragment (tetR-CFP, red) did not translocate from mother to bud; instead, it remained in the mother cell and, thus, independent of spindle position. The distance from the foci on the centric fragment to the spindle midpoint remained constant over time (Figure 4, bottom, closed diamonds), indicating that spindle and centric fragment movements are coupled. In contrast, the distance between the acentric fragment versus either the centric fragment (Figure 4, open diamonds) or spindle midpoint (Figure 4, closed squares) changed over time. Thus, the acentric fragment does not remain tethered to the mitotic spindle.

Microtubule-Based Forces Are Required for Chromosome Fragmentation

Chromosome fragmentation was prevented upon treatment of cells with the microtubule-depolymerizing agent

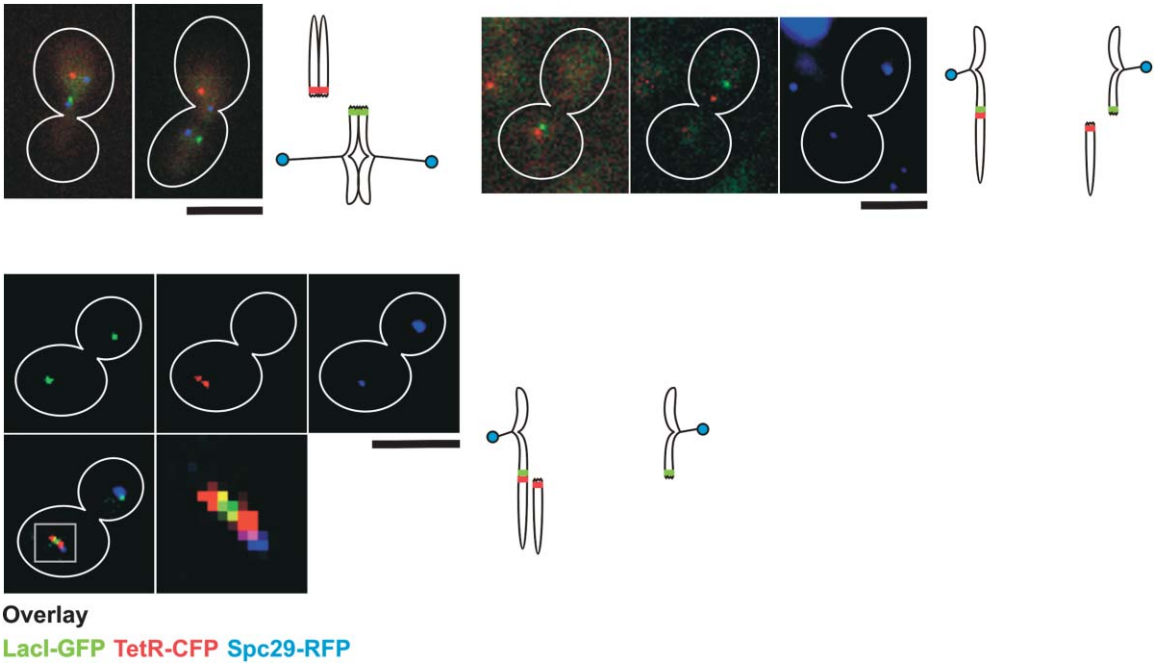

Figure 3. The Morphological Classes of tetR-CFP and lacI-GFP Foci in Live Cells

The centromeric (lacI-GFP) and telomeric (tetR-CFP) sides of the DSB and spindle pole bodies (Spc29-RFP) are indicated in green, red, and blue, respectively. A schematic of the images is provided (right). Separation of operator spots (tetR versus lacI) was observed in cells with unsegregated and segregated sister chromatids.

Upper left: Images of two different cells with spindle poles separated by ~3 μm and single lacI and tetR foci that are separated. Separations such as these composed 86.5% of the total number of foci observed in all strains with separated spots (207/240). The scale bar represents 5 μm.

Upper right: An image of a single cell in which the spindle is elongated (~5.5 μm), and sister chromatids have separated. Individual planes of the Z stack are shown to emphasize the degree of separation. Left, GFP and CFP; middle, GFP and CFP; right, RFP. There are four lacI-GFP and tetR-CFP foci. Sister chromatid separation was observed in 9.6% of cells with separated foci (23/240). The scale bar represents 5 μm.

Lower left: An image of a single cell in which the spindle is elongated (>6 μm); the separated centromeric arrays have segregated to each pole, whereas the telomeric arrays have separated but remain at one spindle pole. This is an example of acentric chromosome fragment loss. Separations of this type were observed in 4.2% of cells that had separated lacI and tetR foci (10/240). The scale bar represents 5 μm.

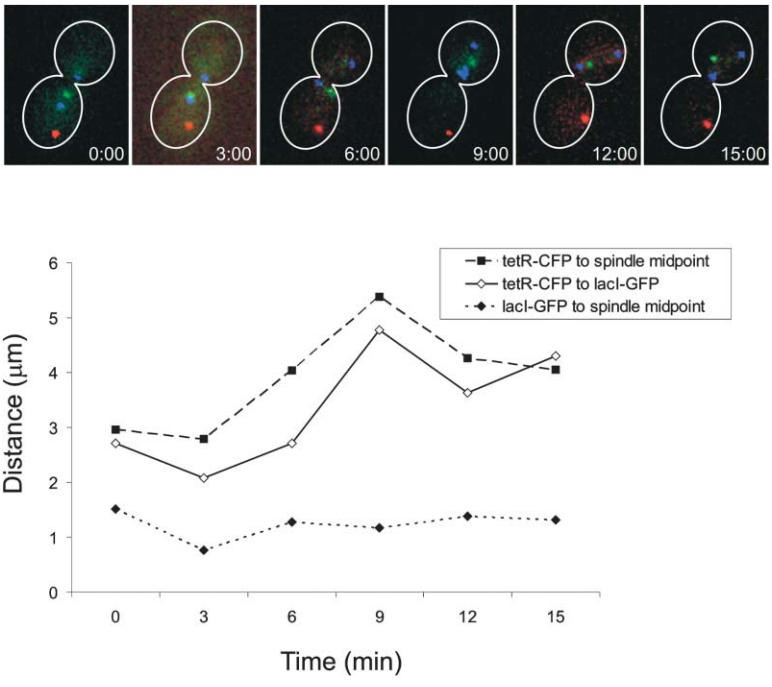

Figure 4. Dynamics of Centric and Acentric Chromosome Fragments

Top: Frames from a 15 min time lapse of a *rad50*-C2S mutant after 2 hr of I-SceI induction. The centromere-proximal arm (lacI-GFP) remained associated with the spindle (Spc29-RFP), whereas the acentric fragment dissociated from the spindle (tetR-CFP, red spot distal from spindle poles). As the spindle migrates from the neck of the budded cell (0:00 min) to the upper bud (9:00 min), the centric fragment behaves accordingly.

Bottom: The distance from the foci on the centric fragment to the spindle midpoint remains constant over time (closed diamonds). In contrast, the distance between the acentric fragment versus either the centric fragment (open diamonds) or spindle midpoint (closed squares) changes over time.

nocodazole without affecting the timing or extent of DSBs (Figures S1 and S3). Less than 1% (1/274) of chromosomes were fragmented in *mre11* mutants in the presence of nocodazole (Figure S3). Upon transfer to media lacking nocodazole, chromosome breakage ensued (9/115 "galactose + nocodazole" to "galactose only"; Figure S3). Thus, microtubule-based forces are required to sever broken chromosomes containing a DSB in the absence of RMX. Once the chromosome was fragmented, the ends remained apart in the presence or absence of microtubules ("galactose" to "galactose + nocodazole"; Figure S3).

Discussion

A single double-strand break in a DNA molecule within solution results in the separation of ends as a consequence of diffusional forces. However, the opportunities for separation of broken chromosome ends are expected to be less because of factors such as histones, nonhistone chromosomal proteins, proteins that interact and repair DSBs, and even nucleus architecture, such as matrix attachment sites. In the present study, we describe a system to distinguish double-strand DNA breaks from chromosomal breaks and address the genetic and physical factors that determine the transition to a CRB. Both the RMX complex and microtubule-mediated forces are important components affecting the transition from DSB to CRB.

Recent studies of the Mre11-Rad50 architecture suggest that RMX has a structural role in bridging two broken molecules during DSB repair [6, 9, 12, 13]. The direct visualization of chromosome breakage in cells lacking RMX demonstrates that its importance in bridging broken DNA strands carries over to the tethering of chromosome ends. Two RMX complexes bound to the DSB ends interact through Cys-X-X-Cys zinc-hook motifs located in the coiled-coil region of the Rad50 protein [6]. Zn-hook domain mutations that do not disrupt Mre11-Rad50 complex formation (*rad50*-C1G, [6]) resulted in levels of chromosome breakage similar to those observed in null mutants (*rad50* and *mre11*) (Figure 2). In contrast, *rad50-C2S* mutants appeared to exhibit increased chromosome breaks (2 hr; *rad50-C2S*; Figure 2), reflecting additional perturbation upon disruption of Mre11-Rad50 complex formation in this mutant. The Zn-hook is therefore critical in prevention of chromosome damage. The lack of chromosome fragmentation in Ku-deficient strains suggests that Ku end binding, regulation of 5′ to 3′ resection [5], and compaction of chromatin in stressed chromosomal regions [14] are not relevant to the appearance of CRBs.

Chromosome breaks in the *mre11* mutants require microtubule-based forces (Figure S3). During metaphase, chromosomes undergo oscillatory movements along the mitotic spindle [15]. Kinetochore microtubules provide sufficient force ($\sim$20 pN/min) [16] to stretch chromatin flanking the centromere beyond the 7-fold compaction of bulk DNA around a nucleosome. Depolymerization of microtubules with antimitotic agents such as nocodazole reduces centromere stretch [16] as well as the incidence of chromosome breaks (Figure S3). In this way, we can estimate that RMX binding at sites of DSB can resist the 20 pN of force that may be propagated along the chromosome axis. The fact that nucleosomes can be displaced when subjected to forces of approximately 20 pN in vitro [17, 18] suggests that microtubule-based forces could indeed disrupt nucleosome interactions that might hold chromosome ends together at sites of DSB in the absence of RMX.

Mutations in *Rad50*, *Mre11*, and *Nbs1* genes have severe consequences in humans and animal models, in which the effects extend from embryonic lethality to various hereditary diseases and a strong predisposition to cancer (reviewed in [19]). Results herein suggest that the Mre11 complex suppresses the formation of chromosome breaks that may lead to the translocations and deletions often associated with cancer. We propose that RMX plays an important role in maintaining chromosome integrity and that changes in its components put the human genome at risk, owing to an increased opportunity for spontaneous or induced chromosome breaks.

Supplemental Data

Detailed Experimental Procedures, three additional figures, and one table are available at http://www.current-biology.com/cgi/content/full/14/23/2107/DC1/.

Acknowledgments

We thank Julian Haase for technical assistance, Drs. Douglas Thrower, Kevin Lewis, and Leanna Topper, who contributed at the early stages of development of this project, Dr. Elaine Yeh for stimulating discussions and wonderful support, and Jim Westmoreland for contributions to the TAFE gel analysis. This work was supported by grants from the National Institutes of Health (GM-32238) and Department of Energy (DE-FG02-99ER62746) to K.S.B. and in part by a Department of Energy interagency award (DE-AI02-99ER62749) to M.A.R.

References

1. Mills, K.D., Ferguson, D.O., and Alt, F.W. (2003). The role of DNA breaks in genomic instability and tumorigenesis. Immunol. Rev. *194*, 77–95.
2. Albertson, D.G., Collins, C., McCormick, F., and Gray, J.W. (2003). Chromosome aberrations in solid tumors. Nat. Genet. *34*, 369–376.
3. Thompson, L.H., and Schild, D. (2002). Recombinational DNA repair and human disease. Mutat. Res. *509*, 49–78.
4. Haber, J.E. (1998). The many interfaces of Mre11. Cell *95*, 583–586.
5. Lee, S.E., Moore, J.K., Holmes, A., Umezu, K., Kolodner, R.D., and Haber, J.E. (1998). Saccharomyces Ku70, mre11/rad50 and RPA proteins regulate adaptation to G2/M arrest after DNA damage. Cell *94*, 399–409.
6. Hopfner, K.P., Craig, L., Moncalian, G., Zinkel, R.A., Usui, T., Owen, B.A., Karcher, A., Henderson, B., Bodmer, J.L., McMurray, C.T., et al. (2002). The Rad50 zinc-hook is a structure joining Mre11 complexes in DNA recombination and repair. Nature *418*, 562–566.
7. Furuse, M., Nagase, Y., Tsubouchi, H., Murakami-Murofushi, K., Shibata, T., and Ohta, K. (1998). Distinct roles of two separable in vitro activities of yeast Mre11 in mitotic and meiotic recombination. EMBO J. *17*, 6412–6425.
8. Moreau, S., Ferguson, J.R., and Symington, L.S. (1999). The nuclease activity of Mre11 is required for meiosis but not for mating type switching, end joining, or telomere maintenance. Mol. Cell. Biol. *19*, 556–566.
9. de Jager, M., van Noort, J., van Gent, D.C., Dekker, C., Kanaar, R., and Wyman, C. (2001). Human Rad50/Mre11 is a flexible complex that can tether DNA ends. Mol. Cell *8*, 1129–1135.

10. Jackson, S.P. (2002). Sensing and repairing DNA double-strand breaks. Carcinogenesis *23*, 687–696.
11. Thrower, D.A., Stemple, J., Yeh, E., and Bloom, K. (2003). Nuclear oscillations and nuclear filament formation accompany single-strand annealing repair of a dicentric chromosome in Saccharomyces cerevisiae. J. Cell Sci. *116*, 561–569.
12. Hopfner, K.P., Karcher, A., Shin, D.S., Craig, L., Arthur, L.M., Carney, J.P., and Tainer, J.A. (2000). Structural biology of Rad50 ATPase: ATP-driven conformational control in DNA double-strand break repair and the ABC-ATPase superfamily. Cell *101*, 789–800.
13. Anderson, D.E., Trujillo, K.M., Sung, P., and Erickson, H.P. (2001). Structure of the Rad50 x Mre11 DNA repair complex from Saccharomyces cerevisiae by electron microscopy. J. Biol. Chem. *276*, 37027–37033.
14. Thrower, D.A., and Bloom, K. (2001). Dicentric chromosome stretching during anaphase reveals roles of Sir2/Ku in chromatin compaction in budding yeast. Mol. Biol. Cell *12*, 2800–2812.
15. Pearson, C.G., Maddox, P.S., Salmon, E.D., and Bloom, K. (2001). Budding yeast chromosome structure and dynamics during mitosis. J. Cell Biol. *152*, 1255–1266.
16. Nicklas, R.B. (1983). Measurements of the force produced by the mitotic spindle in anaphase. J. Cell Biol. *97*, 542–548.
17. Bennink, M.L., Leuba, S.H., Leno, G.H., Zlatanova, J., de Grooth, B.G., and Greve, J. (2001). Unfolding individual nucleosomes by stretching single chromatin fibers with optical tweezers. Nat. Struct. Biol. *8*, 606–610.
18. Brower-Toland, B.D., Smith, C.L., Yeh, R.C., Lis, J.T., Peterson, C.L., and Wang, M.D. (2002). Mechanical disruption of individual nucleosome reveals a reversible multistage release of DNA. Proc. Natl. Acad. Sci. USA *99*, 1960–1965.
19. D'Amours, D., and Jackson, S.P. (2002). The Mre11 complex: At the crossroads of dna repair and checkpoint signalling. Nat. Rev. Mol. Cell Biol. *3*, 317–327.